

POLYANILINE/1-TETRADECANOL COMPOSITES Form-stable PCMS and electrical conductive materials

J. L. Zeng^{1,2}, J. Zhang^{1,2}, Y. Y. Liu^{1,2}, Z. X. Cao^{1,2}, Z. H. Zhang^{1,2}, F. Xu¹ and L. X. Sun^{1*}

¹Materials and Thermochemistry Laboratory, Dalian Institute of Chemical Physics, Chinese Academy of Sciences
Dalian 116023, P. R. China

²Graduate School of the Chinese Academy of Sciences, Beijing 100049, P. R. China

Polyaniline (PANI)/1-tetradecanol (TD) composite materials, a kind of novel composite that can conduct electricity and store thermal energy at the same time, thus possess the ability to endure certain heat shock, were prepared for the first time. FTIR and XRD results showed that there were some interactions existed between PANI and TD. The thermal stability of the composites exhibited both the characteristics of PANI and TD. The DSC experiments showed that the highest phase change enthalpy of the composites could be as 73% as that of TD, indicating it was a good form-stable phase change material. The thermal conductivity of the composites was also improved. The AC (Alternating Current) conductivity of the composites was enhanced to close to that of PANI when the mass fraction of PANI in the composite was increased to 46%. Heat shock experiments showed that the heat shock resistibility of the composite was greatly improved comparing to that of pure PANI.

Keywords: electrical conductive materials, form-stable phase change materials, heat shock resistibility, polyaniline, thermal conductivity

Introduction

Phase change materials (PCMs) are a kind of latent heat storage substance and can be applied in thermal protection field [1]. But the need of encapsulation [2] and the unacceptable low thermal conductivity are the main hindrance to their applications. Form-stable PCMs [2–4], also called shape-stabilized PCMs [5, 6], might be a solution to these questions. In form-stable PCMs, the solid-liquid PCMs are dispersed into the network of the supporting materials [4] so that the encapsulation is omitted. It has been found that the maximum mass percentage for paraffin in the paraffin/HDPE (high density polyethylene) composites without any seepage at a temperature higher than the melting point could be as high as 77% [7]. And by composing paraffin with a thermoplastic elastomer poly(styrene–butadiene–styrene), the obtained shape-stabilized PCM could contain up to 80% of paraffin [8]. Further more, by adding 20% of graphite into a form-stable PCM, its thermal conductivity improved 221% and without the problem of phase separation [6].

Different PCMs should have different congruent supporting materials. However, the reported form stable PCMs were mainly focused on paraffin as PCM and HDPE as supporting material [2–5, 7]. So that it is worthwhile to investigate some other PCMs and supporting materials.

Polyaniline (PANI), a kind of conductive polymer without solid-liquid transition till it is pyrolysed, has

created a promising field of research. PANI has a lot of outstanding properties such as high electrical conductivity, good environment stability, cheap and ease of produce, making it potential candidate for applications in sensors [9], corrosion protection [10], electromagnetic interference shielding materials [11], rechargeable batteries [12], and solar cells [13], etc. Furthermore, although the thermal conductivity of PANI is poor, it has been reported that, by coating the filler with a thin film of PANI, the thermal conductivity of the reaction bed could be improved [14].

The electrical conductivity of PANI is largely depending on the acid doping. However, when the temperature rises to above 40°C, PANI would lose the doped HCl [15] and thus weaken the electrical conductivity [16]. The high photothermal conversion efficiency and poor heat conductivity of PANI can be applied to flash weld conducting polymer nanofibers [17]. However, on conditions that we don't want to weld polymer, strong light may produce high temperature and results in weakened electrical conductivity. If we combine PANI with PCM, the composite material should have the ability to absorb the unwanted thermal energy without appreciable temperature rising and stand up to some thermal shock. As a result, PANI won't lose its electrical conductivity.

In this work, we choose PANI as supporting material and 1-tetradecanol (TD) as the solid/liquid PCM because its melting point is close to 40°C [18]. A series of PANI/TD composite materials was

* Author for correspondence: lxsun@dicp.ac.cn

prepared for the first time. The thermal properties and electrical conductivity were examined. Also investigated was the effect of thermal shock on the electrical conductivity of the composites.

Experimental

Preparation of materials

The composites were prepared as follows. 0.03 g of cetyltrimethyl ammonium bromide (CTAB) was dissolved in 90 mL deionized (DI) water. To this solution, certain amounts of TD, distilled aniline and 1 mL of concentric HCl were added. The mixture was vigorously stirred for 2 h in a 50°C water bath to form an emulsion. The water bath was naturally cooled to room temperature while the stirring continued. As the TD solidified, the emulsion turned to white slurry. The water bath was replaced by an ice-water bath. After the temperature of the mixture was cooled to 0–5°C, 10 mL of ammonium persulfate (APS)-DI water solution was poured into it. The molar ratio of the aniline and APS was fixed to be 1:1. The mixture was stirred vigorously overnight and the ice-water bath was naturally warmed to room temperature. The mixture was left stand still to precipitate the solid materials. The supernate and the solid material floating on the surface were decanted by means of decantation. The precipitation was mixed with DI water and left stand still again. This procedure was repeated till the supernate was nearly colorless. Afterward the mixture was filtered and washed with DI water till the filtrate was totally colorless. The residue was collected and dried in a vacuum desiccator. The raw materials of the series samples were listed in Table 1.

Instrumental methods

IR spectra were recorded on a BRUKER EQUINOX 55 FTIR spectrometer using KBr pellet (400–4000 cm⁻¹). Powder X-ray diffraction (XRD) experiments were carried out on a Rigaku D/max-γb

X-ray diffractometer with monochromatic detector. Copper Kα radiation was used, with a power setting of 50 kV and 200 mA, and a scan rate of 5° min⁻¹.

The energy storage properties of the materials were investigated using differential scanning calorimeter (DSC) (DSC141 SETARAM, France) in the temperature range of –10 to 80°C with the heating rate of 10 K min⁻¹ in nitrogen atmosphere. The masses of the samples used for DSC measurement were about 4–6 mg. The mass fraction of TD in the composite was obtained by dividing the phase change enthalpy of the composites by that of the pure TD. Thermogravimetry/derivative thermogravimetry (TG/DTG) measurements were performed on a Setsys16/18 thermogravimetry analyzer (SETARAM, France) from room temperature to 650°C with the heating rate of 10 K min⁻¹ and N₂ as carrier gas. A Hot Disc thermal constant analyzer was used to obtain the thermal conductivity of the samples at room temperature with a sensor diameter of 2.001 mm. The grinded sample was pressured to form two cylinders with the diameter of 13 mm under 2 MPa. The sensor was sandwiched by the two cylinders and fixed by a clamp.

About 0.1 g of grinded sample was pressured into a disc in the diameter of 13.10 mm under 2 MPa. In order to understand the alternating current (AC) conductivity, the disc was sandwiched between two copper electrodes. The AC impedance of the samples was measured on a Zahner Elektrik IM6e electrochemical workstation in the frequency range of 0.1 Hz and 10 KHz applying the method of two electrodes without buffer. The specific AC conductivity was calculated from AC impedance according to:

$$\sigma(f) = \frac{1}{|Z^*(f)|} \frac{t}{A} \quad (1)$$

where A is the contact area which is equal to the cross sectional area of the disc, t is the sample thickness and $Z^*(f)$ is the complex impedance of the sample as a function of frequency [19].

Table 1 The raw materials ratio when preparing the samples and the data of DSC experiments results

Sample	TD	S1	S2	S3	S4	S5	S6	S7	PANI
TD/g		1.6	1.4	1.2	1.0	0.8	0.6	0.4	/
Aniline/g	/	0.4	0.6	0.8	1.0	1.2	1.4	1.6	2.0
$T_{\text{onset}}/^{\circ}\text{C}$	34.85	33.54	33.77	33.25	32.74	33.38	34.23	34.85	
$T_{\text{peak}}/^{\circ}\text{C}$	39.34	39.80	36.31	38.96	37.14	36.84	37.22	36.03	
Phase change enthalpy/J g ⁻¹	221.23	162.97	162.64	133.62	119.14	82.39	66.14	35.23	
TD mass fraction/%*	100	73.64	73.49	60.37	58.83	37.23	29.89	15.92	/

*The TD mass fraction of the samples was calculated by dividing the phase change enthalpy of samples by that of pure TD

Results and discussion

The IR spectra profiles of the PANI, TD and the composite materials are shown in Fig. 1. The spectrum of the pure PANI shows the typical characteristics of HCl doped PANI [20] and the assignments of each absorption peak are listed in Table 2. Also listed in Table 2 is the absorption peaks assignment of pure TD. By comparing the spectra of PANI, TD and composites, we can find that the spectra of the composites are superposed from PANI and TD, and the composites are the mixture of TD and PANI. All absorption peaks in the spectra of PANI and TD can find its corresponding band in the spectra of the composites. The intensity of the characteristic peaks of TD was intensified while that of PANI was weakened as the mass fraction of TD increased. For the composites, there is no significant band shifting occurs comparing to PANI and TD except the C–C vibrations of quinoid ring and benzene ring. In the composites, these two absorptions blue shifted from 1564 and 1483 cm^{-1} to about 1575 and 1490 cm^{-1} , respectively, which means that a certain extent of interactions exist between PANI and TD. These

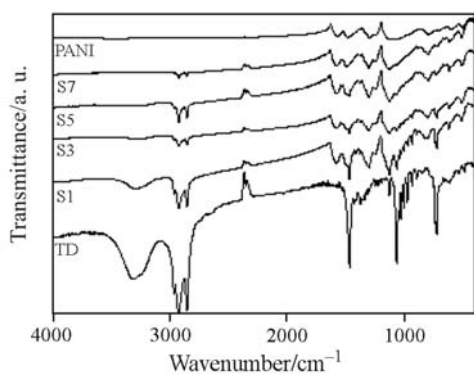


Fig. 1 IR spectra of the PANI, TD and the composite

Table 2 IR Vibrational Frequencies of Pure PANI and TD

Sample	Interatomic bond	Vibrational frequency/ cm^{-1}
PANI	C–C of quinoid ring	1564
	C–C of benzene ring	1483
	C–N	1294
	C–H of benzene ring	1240
	C–H of quinoid ring	1118
	benzene and quinoid ring C–H	792
TD	O–H	3300
	C–H	2918, 2848, 1463
	C–O	1062
	–CH ₃ - rocking vibration	719

blue-shifts can be explained as follows. As the TD was introduced into the reaction system, aniline became adsorbed on the surface of the TD granule [21]. Polymerization initiated firstly on the surfaces of these granules [22, 23]. This led to the adhesion of the polymer to the TD granule and thus the constrained growth of the polymer chains around the granule [24]. Such adhesion and constraining of the polymer chains will increase the force coefficient of the C–C bonds of the quinoid and benzene ring, resulting in the blue-shifting of these two bands.

The ordered structures of the PANI, TD and the composites were studied by powder X-ray diffraction (Fig. 2). The XRD pattern of the PANI agrees well with references [25, 26], indicating the PANI is in the form of conductive emeraldine salt (ES). The patterns of composites are mainly similar to that of TD except the diffractions near $2\theta=26^\circ$ are originated from PANI. All diffraction peaks of pure TD can find their corresponding peaks in the patterns of composites. The shape and the width of the peaks have not changed evidently. This observation suggests that the polymerization of aniline at the surface of the TD granule does not destroy the crystalline order of the TD. Yet there are some differences existed by careful observing the patterns of the PANI, TD and the composites. First, the two diffractions of the PANI at 2θ angles around 15 and 20° are disappeared in the composites. The peak at 20° might be covered by TD due to its strong diffraction near this angle, but the disappearing of peak at 15° we think is caused by the interactions between PANI and TD, which has been demonstrated by IR inspection. Second, in TD, the intensity of diffractions at 2θ angles around 30 and 35° is very weak comparing to other diffractions. However, in the composites, these two diffractions are relatively stronger diffractions. More detailed work on the cause of these differences is undertaking but it can be seen that the intensity of these two diffractions become weaken as the TD mass fraction decreased in the composites, indicating the crystallinity of the composites decreased.

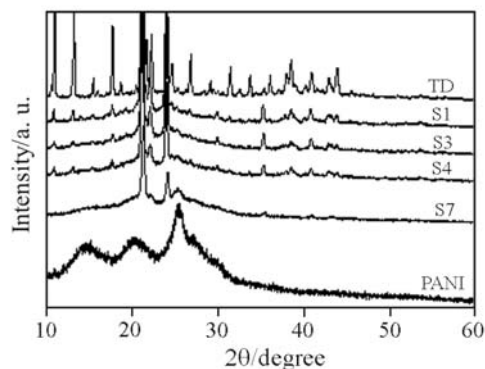


Fig. 2 XRD patterns of the PANI, TD and the composite

When the composites were heated to 50°C, a temperature higher than the melt point of TD, no liquid could be found and the samples could maintain its shape and will not collapse. This means that the composites are form-stable PCMs. When the composites are utilized as PCMs, the most important property is the ability to store thermal energy. The thermal energy storage properties of pure TD have been reported in detail [18]. Here the phase change enthalpy of the composites and TD, along with the temperature of phase transition, obtained from DSC experiments, are listed in Table 1. It can be seen that the phase transition temperature of the composites is a little bit lower to that of pure TD, which is the characteristic of mixture. Considering the information obtained by IR and DSC experiments, we can conclude that the interaction between PANI and TD is just physical adsorption.

The data of phase change enthalpy show that S1 has the highest phase change enthalpy (162.97 J g^{-1}) in the composites. The phase change enthalpy of S2 is 162.64 J g^{-1} and is very close to that of S1. The highest phase change enthalpy of the composites is larger than or comparable to the form-stable PCMs reported in references. Obviously the composite can be viewed as a good form-stable PCM. Also can be seen from the table is that the highest TD mass fraction in the form-stable PCM is about 73% and will not increase anymore even the raw materials ratio is higher than this value. The reason can be interpreted as follows. In the reaction mixture, the amount of the surfactant, CTAB, is certain and the maximal amount of TD that can be emulsified by CTAB is certain. When the TD mass in the mixture exceed this value, the exceeded TD would form big granule floating on the water surface and be decanted even it has been composed with PANI. We have applied higher concentration of CTAB to prepare the form-stable PCM with high mass fraction of TD. The scum was decreased but the mixture was too emulsified to filtrate. So in the present system, the highest TD mass fraction is about 73%.

When the ratio of TD/(TD+aniline) of the composites is lower than 70%, the phase change enthalpy of the form-stable PCMs is decreased linear with the decreasing of the ratio (Fig. 3). This means that we can prepare the form-stable PCM with admirable phase change enthalpy (TD mass fraction), which is crucial when the composites are used as conductive materials.

The thermal stability of the PANI, TD and the composites is described in Fig. 4. The TG curve of PANI shows a three-step mass loss process and agrees with reference [27]. The composites with lower PANI content (S1, S2, S3 and S4) exhibit three peaks in the

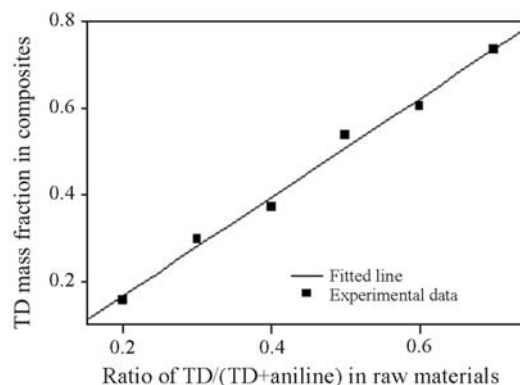


Fig. 3 Relation between the raw materials ratio of TD/(TD+aniline) and the enthalpy ratio of form-stable PCM/Pure TD

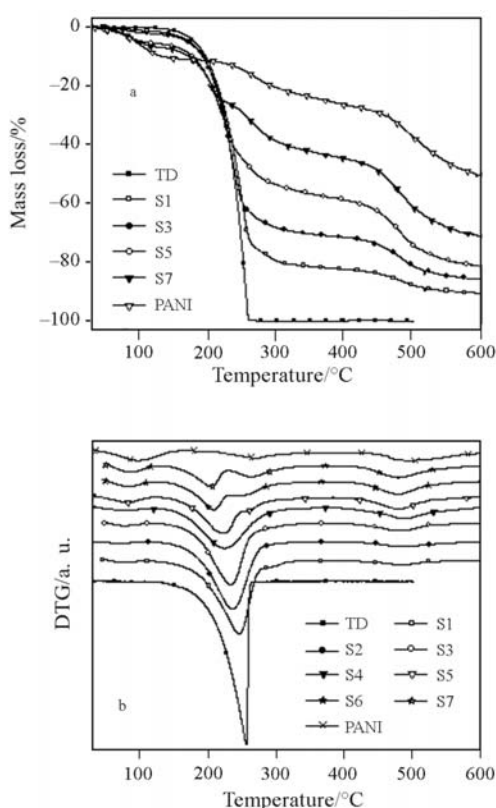


Fig. 4 a – TG and b – DTG curves of the PANI, TD and the composites

DTG curves (Fig. 5b), indicating they also show the three-step mass loss processes similar to that of PANI. The first and the third step of mass loss of PANI are related to the release of moisture and doped HCl from the surface of PANI and the decomposition of PANI chains [28], the corresponding mass loss regions are also appeared in composites and the mass loss rate is increased as the TD mass fraction decreased. The second step of mass loss of PANI is related to the further release of the doped HCl [28]. Its temperature range is overlapped with the mass loss

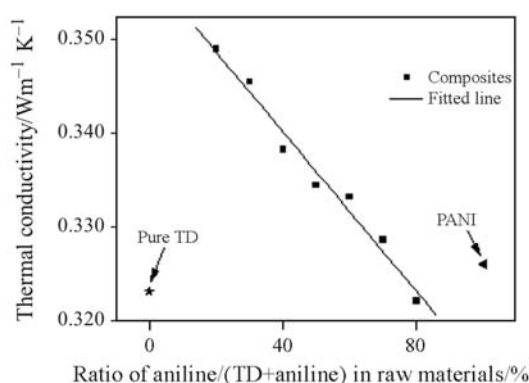


Fig. 5 Thermal conductivity of the composite as a function of ratio of aniline/(TD+aniline) in raw materials. Also showed is the thermal conductivity of TD and PANI

region of TD. As a result, the mass loss ratio of S1, S2, S3 and S4 at the second step is increased as the TD mass fraction increased. However, the DTG curves of the composites with higher PANI content (S5, S6 and S7) show four peaks. The second and third peaks are very close in S5. But the distance between these two peaks is enlarged gradually as the PANI content increased and is totally separated in S7. The difference of thermal degradation behavior between higher and lower PANI content composites is because that, in lower PANI content composites, the release of doped HCl of the PANI at the second step has been completed before the TD was totally lost, so that there is only one peak appeared in the DTG curve. On the other hand, as the PANI content increased, the release of doped HCl from inner PANI becomes difficult and would occur at higher temperature. As a result, a new peak exclusively implies the release of doped HCl from the inner PANI appeared in the DTG curve.

Figure 5 shows the thermal conductivity of the PANI, TD and the composites. The figure shows that, except S7, the thermal conductivity of all other composites is higher than pure TD. This is an appreciative result for the composites to be applied as PCMs. By introducing about 30% of PANI into the composite, the thermal conductivity of the composite increased nearly 10%, from around 0.32 W mK^{-1} to about 0.35 W mK^{-1} . However, further increasing of PANI resulted in lower thermal conductivity. PANI can be viewed as thermal conductivity enhancing filler in the composites. At low concentration of aniline in the reaction mixture, the reaction rate was slow, resulting in more crystalline PANI with stronger thermal conductivity enhancement. As the concentration of aniline in the reaction mixture became higher, the reaction rate increased and resulted in less crystalline PANI, thus weakened the thermal conductivity enhancement. The thermal conductivity of S7 is lower than that of TD and

PANI could be attributed to the low thermal conductivity of PANI caused by the low crystallinity of PANI and the interface thermal resistance between the TD and the PANI.

The specific AC conductivity of the PANI, TD and the composites are depicted in Fig. 6a. For TD, there is a direct current plateau existed and followed by a frequency-dependent region as frequency increases, indicating TD is a disorder solid. Whereas for composites and PANI, the frequency-dependent region is disappeared, implying the conductive network has been formed [29]. The curves of the composites with high PANI mass fraction are overlapped because their AC conductivity is similar. But Fig. 6b, which shows the specific AC conductivity of the PANI, TD and the composites at 0.1 Hz, shows the change of the AC conductivity of the composites clearly. The figure revealed that TD is insulator. When TD was composed with 30% of PANI, the specific AC conductivity at 0.1 Hz is suddenly jumped to about 0.01 S m^{-1} . We find that Fig. 6b is similar to the results reported in the reference [30], in which the percolation threshold value was in the range of 7 and 18%. Obviously, the percolation threshold of the composites in this work should be lower than 30%. Since the purpose of this paper is to investigate form-stable PCMs and electrical conductive materials with heat shock resistibility, we need not know the exact percolation threshold. When

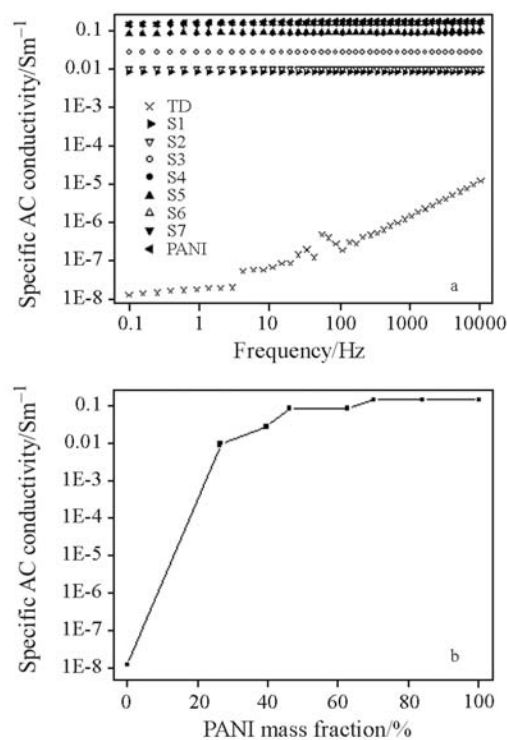


Fig. 6 Specific AC conductivity of the PANI, TD and composites. a – as a function of frequency, b – as a function of PANI mass fraction at 0.1 Hz

the mass fraction of PANI in the composite was increased to 46%, the conductivity is enhanced to near 0.1 S m^{-1} , which is close to that of PANI. More increasing of PANI mass fraction won't result in significant conductivity enhancement. It means when the composite is used as electrical conductive material, the PCM mass fraction in it can be as high as about 54%.

In order to investigate the ability of the composite materials to withstand heat shock, the discs of the S6 and PANI were placed in an oven of 170°C for 10 s and cooled to room temperature in ambient environment. The AC conductivity of the discs was measured after 15 and 30 circles of heating and cooling. The results are shown in Fig. 7. For S6, the conductivity decreased about 20% after 30 cycles of heating/cooling, from 0.15 to 0.12 S m^{-1} . However, after 30 cycles, sharp decrease in conductivity of the PANI from 0.15 to 0.05 S m^{-1} , nearly 70%, is observed. The PANI would lose the doped HCl and moisture when it is heated to beyond 40°C [15]. The loss of HCl would reduce the size of conducting grains, and thus reduce the conductivity [31, 32]. But for the composites, TD can absorb heat by changing from solid to liquid and maintaining the temperature under its melting point before it is fully melted. As a result, the loss of HCl and moisture will not occur. So that it is the phase change property of the TD makes the composites have the ability to withstand heat shock.

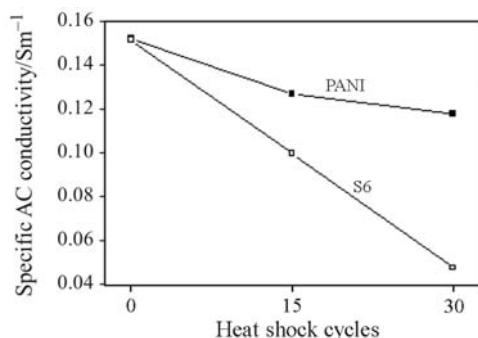


Fig. 7 Effect of heat shock cycles on the specific AC conductivity of S6 and PANI at 0.1 Hz

Conclusions

PANI/TD composite materials were prepared via in-situ polymerization. TD was used as PCM and PANI as conductive material. The composites can be applied as either electrical conductive materials or form-stable PCMs. The composites possess the ability to endure certain heat shock when the composites were used as conductive materials. The AC conductivity of the composites was enhanced to near that of PANI when the mass fraction of PANI in the composite was increased to 46%. DSC experiments

indicated that the highest phase change enthalpy of the composites could be as 73% as that of TD and the phase change enthalpy of the composites increased as the TD mass fraction of the composites increased. The thermal conductivity of the composites with 73% TD was about 10% higher than that of pure TD and decreased as TD mass fraction decreased. FTIR and XRD results showed that there were some interactions existed between PANI and TD. The thermal stability of the composites exhibited both the characteristics of PANI and TD.

Acknowledgements

The authors gratefully acknowledge the National Natural Science Foundation of China for financial support to this work under Grant NSFC No. 20473091, 50671098 and 20573112.

References

- 1 S. V. Garimella, *Microelectron. J.*, 37 (2006) 1165.
- 2 Y. P. Zhang, K. P. Lin, R. Yang, H. F. Di and Y. Jiang, *Energ. Buildings*, 38 (2006) 1262.
- 3 H. Inaba and P. Tu, *Heat Mass Transfer*, 32 (1997) 307.
- 4 H. Ye and X. S. Ge, *Sol. Energ. Mat. Sol. C.*, 64 (2000) 37.
- 5 Y. B. Cai, Y. Hu, L. Song, H. D. Lu, Z. Y. Chen and W. C. Fan, *Thermochim. Acta*, 451 (2006) 44.
- 6 Y. P. Zhang, J. H. Ding, X. Wang, R. Yang and K. P. Lin, *Sol. Energy Mater. Sol. Cells*, 90 (2006) 1692.
- 7 A. Sari, *Energy Convers. Manage.*, 45 (2004) 2033.
- 8 M. Xiao, B. Feng and K. C. Gong, *Energ. Convers. Manage.*, 43 (2002) 103.
- 9 S. Virji, R. B. Kaner and B. H. Weiller, *J. Phys. Chem. B*, 110 (2006) 22266.
- 10 L. Zhong, S. H. Xiao, J. Hu, H. Zhu and F. X. Gan, *Corros. Sci.*, 48 (2006) 3960.
- 11 M. A. Soto-Oviedo, O. A. Araújo, R. Faez, M. C. Rezende and M. A. De Paoli, *Synth. Met.*, 156 (2006) 1249.
- 12 G. Torres-Gómez, E. M. Tejada-Rosales and P. Gómez-Romero, *Chem. Mater.*, 13 (2001) 3693.
- 13 S. X. Tan, J. Zhai, M. X. Wan, Q. B. Meng, Y. L. Li, L. Jiang and D. B. Zhu, *J. Phys. Chem. B*, 108 (2004) 18693.
- 14 L. J. Wang, D. S. Zhu and Y. K. Tan, *Adsorption*, 5 (1999) 279.
- 15 R. Gangopadhyay, A. De and G. Ghosh, *Synth. Met.*, 123 (2001) 21.
- 16 Ö. Yavuz, M. K. Ram, M. Aldissi, P. Poddar and S. Hariharan, *J. Mater. Chem.*, 15 (2005) 810.
- 17 J.X. Huang and R.B. Kaner, *Nat. Mater.*, 3 (2004) 783.
- 18 J. L. Zeng, L. X. Sun, F. Xu, Z. C. Tan, Z. H. Zhang, J. Zhang and T. Zhang, *J. Therm. Anal. Cal.*, 87 (2007) 369.
- 19 C. A. Martin, J. K.W. Sandler, M. S. P. Shaffer, M.-K. Schwarz, W. Bauhofer, K. Schulte and A. H. Windle, *Compos. Sci. Technol.*, 64 (2004) 2309.
- 20 H. B. Xia, J. Narayanan, D. M. Cheng, C. Y. Xiao, X. Y. Liu and H. S. O. Chan, *J. Phys. Chem. B*, 109 (2005) 12677.

POLYANILINE/1-TETRADECANOL COMPOSITES

- 21 X. T. Zhang, J. Zhang, R. M. Wang and Z. F. Liu, *Carbon*, 42 (2004) 1455.
- 22 A. Malinauskas, *Polymer*, 42 (2001) 3957.
- 23 S. Fedorova and J. Stejskal, *Langmuir*, 18 (2002) 5630.
- 24 W. Feng, X. D. Bai, Y. Q. Lian, J. Liang, X. G. Wang and K. Yoshino, *Carbon*, 41 (2003) 1551.
- 25 S. Quillard, G. Louarn, S. Lefrant and A. G. MacDiarmid, *Phys. Rev. B*, 50 (1994) 12496.
- 26 L. J. Pan, L. Pu, Y. Shi, T. Sun, R. Zhang and Y. D. Zheng, *Adv. Funct. Mater.*, 16 (2006) 1279.
- 27 X. M. Sui, Y. Chu, S. X. Xing, M. Yu and C. Z. Liu, *Colloid Surf. A-Physicochem. Eng. Asp.*, 251 (2004) 103.
- 28 P. Ghosh, S. K. Siddhanta, S. R. Haque and A. Chakrabarti, *Synth. Met.*, 123 (2001) 83.
- 29 A.N. Papathanassiou, I. Sakellis, J. Grammatikakis, E. Vitoratos, S. Sakkopoulos and E. Dalas, *Synth. Met.*, 142 (2004) 81.
- 30 H. Yoshikawa, T. Hino and N. Kuramoto, *Synth. Met.*, 156 (2006) 1187.
- 31 J. Prokeš and J. Stejskal, *Polym. Degrad. Stab.*, 86 (2004) 187.
- 32 X. H. Lu, C. Y. Tan, J. W. Xu and C. B. He, *Synth. Met.*, 138 (2003) 429.

Received: April 5, 2007

Accepted: June 12, 2007

DOI: 10.1007/s10973-007-8495-8